Int J Biometeorol (2016) 60:1389–1403
DOI 10.1007/s00484-015-1132-5

ORIGINAL PAPER

Spatiotemporal variability and predictability of Normalized Difference Vegetation Index (NDVI) in Alberta, Canada

Rengui Jiang[1] · **Jiancang Xie**[1] · **Hailong He**[2] · **Chun-Chao Kuo**[3] · **Jiwei Zhu**[1] · **Mingxiang Yang**[4]

Received: 24 May 2015 / Revised: 22 November 2015 / Accepted: 27 December 2015 / Published online: 14 January 2016

Abstract As one of the most popular vegetation indices to monitor terrestrial vegetation productivity, Normalized Difference Vegetation Index (NDVI) has been widely used to study the plant growth and vegetation productivity around the world, especially the dynamic response of vegetation to climate change in terms of precipitation and temperature. Alberta is the most important agricultural and forestry province and with the best climatic observation systems in Canada. However, few studies pertaining to climate change and vegetation productivity are found. The objectives of this paper therefore were to better understand impacts of climate change on vegetation productivity in Alberta using the NDVI and provide reference for policy makers and stakeholders. We investigated the following: (1) the variations of Alberta's smoothed NDVI (sNDVI, eliminated noise compared to NDVI) and two climatic variables (precipitation and temperature) using non-parametric Mann-Kendall monotonic test and Thiel-Sen's slope; (2) the relationships between sNDVI and climatic variables, and the potential predictability of sNDVI using climatic variables as predictors based on two predicted models; and (3) the use of a linear regression model and an artificial neural network calibrated by the genetic algorithm (ANN-GA) to estimate Alberta's sNDVI using precipitation and temperature as predictors. The results showed that (1) the monthly sNDVI has increased during the past 30 years and a lengthened growing season was detected; (2) vegetation productivity in northern Alberta was mainly temperature driven and the vegetation in southern Alberta was predominantly precipitation driven for the period of 1982–2011; and (3) better performances of the sNDVI-climate relationships were obtained by nonlinear model (ANN-GA) than using linear (regression) model. Similar results detected in both monthly and summer sNDVI prediction using climatic variables as predictors revealed the applicability of two models for different period of year ecologists might focus on.

Keywords Variability · Smoothed NDVI (sNDVI) · sNDVI-climate relationships · Predictive model

✉ Rengui Jiang
jrengui@163.com

✉ Jiancang Xie
jcxie@mail.xaut.edu.cn

✉ Hailong He
hailong.he@hotmail.com

[1] State Key Laboratory Base of Eco-hydraulic Engineering in Arid Area, Xi'an University of Technology, Xi'an 710048, China

[2] College of Natural Resources and Environment, Northwest A&F University, Yangling 712100, China

[3] Department of Civil & Environmental Engineering, University of Alberta, Edmonton T6G 1H9, Canada

[4] State Key Laboratory of Simulation and Regulation of Water Cycle in River Basin, China Institute of Water Resources and Hydropower Research, Beijing 100038, China

Introduction

Climate change has been proven to affect the plant growth, vegetation productivity, water resources, and socio-economic systems of many regions worldwide, and the impacts will likely to continue to increase in the twenty-first century (Piao et al. 2010; Tanzeeba and Gan 2012). The Fifth Assessment Report (AR5) of the Intergovernmental Panel on Climate Change (IPCC) showed that the global surface air temperature had increased by 0.85 ± 0.21 °C from 1880 to 2012. High confident evidences indicated that the period from 1983 to 2012 was likely the warmest 30-year period of the last 800 years in the Northern Hemisphere (NH). A strong evidence of global warming was the worldwide melting and increasing global anthropogenic

CO_2 emissions. For instance, the snow cover in the NH had decreased from 1.6 % per decade in March to 11.7 % per decade in June between 1947 and 2012. Total annual anthropogenic greenhouse gas (GHG) emissions had grown on average by 1.0 $GtCO_{2eq}$ per year from 2000 to 2010 (IPCC 2013). Global warming had been proven to affect the vegetation productivity, and the changes of snow cover and anthropogenic GHG emissions had shown to enhance productivity of terrestrial and biological systems over the past several decades in terms of widened vegetation cover and lengthened growing season in northern middle and high latitudes (Nemani et al. 2003). As one of the most popular vegetation indices used for monitoring short- and long-term variations of plant growth and terrestrial vegetation productivity (Jahan and Gan 2011), Normalized Difference Vegetation Index (NDVI) has been widely used to evaluate the dynamic response of vegetation to changes in climatic variables at both global (de Jong et al. 2011; Ichii et al. 2002) and regional scales (Chuai et al. 2012; Jahan and Gan 2011; Canon et al. 2011; Latifovic et al. 2005). NDVI can be used as a proxy of plant growth and vegetation productivity, partly because the amount of solar radiation reflected by vegetation is related to the wavelength, the chlorophyll, leaf interior tissues, and water content in vegetation (Dorigo et al. 2012; Wang et al. 2003).

There have been studies on the variations of NDVI and its relationships with hydroclimatic variables, such as precipitation and temperature. Besides, soil moisture status also determines the plant growth and vegetation productivity. However, the lack and limitation of long-term soil moisture observations make it difficult to establish links between changes in soil moisture availability and NDVI. Regional responses of vegetation at northern latitudes to moisture variability have typically been inferred indirectly by analyzing correlations between NDVI and climatic variables, mainly precipitation and temperature (Barichivich et al. 2014; Jahan and Gan 2011; Gómez-Mendoza et al. 2008; Prasad et al. 2005). For example, using NDVI from the Pathfinder Advanced Very High Resolution Radiometer (AVHRR) satellite sensors of National Oceanic and Atmospheric Administration (NOAA), Ichii et al. (2002) found significant correlations between interannual NDVI and temperature variability during the growing season in the northern middle and high latitude regions, and between NDVI and precipitation in semiarid regions. With a rise in temperature, NDVI increased in northern middle and high latitude regions but decreased in southern semiarid regions due to decreased precipitation. Wang et al. (2003) investigated the temporal responses of NDVI data to precipitation and temperature during 1989–1997 in Kansas, USA. The results showed that the mean NDVI during growing season was highly correlated to precipitation and positively correlated to temperature in the early and late growing season, but only weakly and negatively correlated with temperature in the midst of growing season. More recently, Gómez-Mendoza et al. (2008) studied the NDVI variations in terms of precipitation anomalies and assessed the onset and length of greening period based on the NDVI-precipitation relationship for the state of Oaxaca in southern Mexico.

Based on the above previous studies, the general strong correlations between NDVI and climatic variables indicated the possibility to predict changes in NDVI with respect to changes in climatic conditions. However, few studies have been found to investigate the credibility of predicting vegetation productivity (NDVI as a proxy) using climatic variables as predictors based on the strong relationships between NDVI and climatic variables under climate change. The paper focus to investigate the links of monthly and seasonal smoothed NDVI (sNDVI) with precipitation and temperature to reveal the impacts of climate on the Alberta's vegetation productivity, and to explore the possibly predictability of terrestrial vegetation productivity using climatic variables as potential predictors based on the correlations between sNDVI and climatic variables. The primary objectives of this study are to (1) investigate the trend magnitudes, spatial and temporal variations of sNDVI for the period of 1982–2011 in Alberta using the Mann-Kendall test and Thiel-Sen's slope; (2) study the relationships between monthly and summer sNDVI and climatic variables (precipitation and temperature); and (3) develop two sNDVI predictive models including a linear regression model and an artificial neural network calibrated by genetic algorithm (ANN-GA) to assess the predictability of vegetation productivity using climatic variables as predictors.

Materials and methods

Study area

Alberta is cutoff at the southwest corner by the Canadian Rocky Mountains, and it is located between 49°N-60°N latitude and 110°W-120°W longitude, as shown in Fig. 1 (Jiang et al. 2014). It has a land area of about 661, 000 km^2, of which more than one third is farmland and the landscapes vary from glacial mountain lakes and rolling foothills to vast boreal forests in the north and grassland in the south (Jiang et al. 2015). It has a semiarid, continental climate partly because it is located in the rain shadow of the Canadian Rocky Mountains, which block the moist westerly winds from the Pacific Ocean, causing orographic precipitation to occur on the windward side. Therefore, located at the leeward side, Alberta is relatively dry, with an annual mean precipitation ranging from about 400 mm to over 500 mm in the north, and from less than 350 mm to about 450 mm in the south (Mwale et al. 2009). The hydrological conditions of Alberta are multifarious because of the diversity of its

Fig. 1 Location of Alberta

physiographic features and climate, which vary seasonally and regionally (Gordon et al. 2005).

Climate and NDVI data

As one of the three Canadian Prairies provinces and the fourth largest province in Canada, Alberta has the best spatial coverage of climate observing stations with long and reliable historical climate data that are crucial for variation analysis (Hopkinson et al. 2012; Vincent and Gullett 1999). High quality precipitation and temperature data used in the study were obtained from the Canadian Gridded Temperature and Precipitation Anomalies (CANGRD) dataset, which have undergone rigorous quality control and have been adjusted for inhomogeneities due to station relocation and station automation, changes in instrumentation, station condition, and environment (Vincent et al. 2012). The CANGRD data sets have a 50 km × 50 km spatial resolution and a polar stereographic projection for the period of 1982–2011. They were gridded from 210 long-record temperature stations (Vincent and Gullett 1999) and 491 precipitation stations across Canada (Mekis and Vincent 2011), which were normalized for individual station departure from the reference period of 1960–1990 and divided by the 1960–1990 period mean, and then generated to gridded data sets (Jiang et al. 2014; Zhang et al. 2000). Therefore, CANGRD data sets are among the best available climate data for Alberta, which have already been used in several studies, e.g., Jiang et al. (2015); Jiang et al. (2014); Vincent et al. (2012); Mekis and Vincent (2011); Zhang et al. (2000).

NDVI is defined as the difference in reflectance between visible (VIS) and near infrared (NIR) sections of solar spectrum (Eq. 1), ranging from −1.0 to 1.0. Bigger NDVI represents larger difference between the NIR and VIS bands, which essentially indicates greener, denser, or more vigorous vegetation. Positive values represent vegetated conditions, while negative and near zero values represent non-vegetated conditions (e.g., water, snow, barren surfaces) (Chuai et al. 2012; Dorigo et al. 2007).

$$\mathrm{NDVI} = (\mathrm{NIR}-\mathrm{VIS})/(\mathrm{NIR}+\mathrm{VIS}) \quad (1)$$

NDVI used in the study was derived from NOAA-AVHRR dataset based on the observations of seven polar-orbiting satellites, from NOAA-7 launched on June 23, 1981 to NOAA-19 launched on June 2, 2009 (Kogan et al. 2013; Kogan et al. 2011). Because NDVI could be affected by noises resulted from atmosphere constituents (e.g., cloud, aerosol, and water vapor), unusual event (e.g., volcanic), view geometry, pre- and post-launch calibrations, satellite orbital drift, and sensor degradation, which reduce the reliability of NDVI, a sNDVI data set developed by Kogan et al. (2011) was used in the study. sNDVI has characteristics of global coverage at 16 km resolution and weekly composite, and it is appropriate for the global or regional analysis of plant growth and vegetation productivity (de Jong et al. 2011). In our study, using the

weekly maximum composite from 1982 to 2011, sNDVI was aggregated to monthly values and regridded to a resolution of 0.5° × 0.5°.

Trend and correlation analysis

Mann-Kendall and Thiel-Sen methods

Trends of sNDVI, precipitation, and temperature were calculated using the non-parametric Mann-Kendall monotonic method at the 5 % significant level, which has been widely used in detecting monotonic trends of climatic variables time series. To eliminate the influence of serial correlation on the trend detection of those data, the Mann-Kendall test was used before the process of trend-free prewhitening (TFPW). However, it essentially produced the same results (Yue et al. 2002). As found by Bayazit and Önöz (2007) which showed that the prewhitening procedure was not necessary for large data samples ($n \geq 50$) or time series with large trend magnitudes.

The trend magnitude identified by the Mann-Kendall method is estimated using Thiel-Sen approach, represented by Sen's slope β, which is defined as the median of all possible combinations for the whole data set, as shown in Eq. 2 (Yue et al. 2002; Gan 1998).

$$\beta_k = \text{median}\left[\left(X_{jk} - X_{ik}\right)/(j-i)\right], \quad i, j \in [1, n] \tag{2}$$

where $X = \{x_1, \cdots, x_i \cdots x_n\}$, n is the length of X, k is the number of grid points, and $i < j$. β is the estimated trend magnitude of X. Positive and negative values of β indicate increasing and decreasing trend magnitudes, respectively.

Mann-Kendall test was applied to investigate the trends of summer (from June to August) sNDVI at the 5 % significant level for each grid point (at resolution of longitude-latitude 0.144° × 0.144°) from 1982 to 2011 in Alberta. Sen's slope was used to analyze the trend magnitudes of monthly sNDVI and climatic variables including precipitation and temperature, and to investigate the trend magnitudes of summer sNDVI for each grid point.

Correlation analysis

Correlation analysis is commonly used to reveal the relationship between two variables. The resulting values called correlation coefficients range from −1 to +1. A correlation coefficient of +1 indicates that two variables are perfectly positively related, while a correlation coefficient of −1 indicates that two variables are perfectly negatively related. Correlation analysis was used in this study to investigate the relationships between Alberta's monthly sNDVI and precipitation (temperature), and between summer sNDVI and precipitation (temperature) for each grid point in Alberta. The spatial patterns of trend magnitudes of summer sNDVI and correlation coefficients between summer sNDVI and precipitation (temperature) for each grid point in Alberta were investigated using contour by Kriging gridding method.

To provide more details of relationships between summer sNDVI and precipitation (temperature), we further investigated the temporal series of mean summer sNDVI, total summer precipitation, and mean summer temperature. The raw data were standardized using z score normalization method before analysis.

sNDVI predictive models

A linear regression model and an ANN-GA model were developed to predict sNDVI using climatic variables as potential predictors for the period of 1982–2011 in Alberta. Because sNDVI was strongly correlated to local precipitation and temperature, it is possibly to predict sNDVI using precipitation and temperature as potential predictors. Previous studies, such as Barichivich et al. (2014) and Gómez-Mendoza et al. (2008) showed that there was often a lag between maximum vegetation productivity and climatic variables. To reveal the lag effect of climatic variables to vegetation productivity, we tested several combinations of sNDVI and climatic variables with 1- or 2-month lag time in the sNDVI predictive models, and the combination of monthly sNDVI and climatic variables with stronger correlations is thought to be more suitable for the predictive models. Based on the correlation analysis of summer sNDVI and climatic variables, we tested three combinations including July sNDIV and June climatic variables, August sNDVI and July climatic variables at 1-month lag time, and August sNDVI and June climatic variables at 2-month lag time. Preliminary analysis showed that August sNDVI was stronger correlated to the July climatic variables than other two combinations, so August sNDVI had been used as the predictand, July precipitation and temperature had been used as predictors for both linear (multivariate regression) and nonlinear (ANN-GA) models. Twenty-four years (1982–2005) of the data were used to calibrate the models and 6 years (2006–2011) of data were used to validate the models.

Linear regression model

Equation 3 shows the linear regression model between sNDVI and the predictors.

$$\text{sNDVI} = k_0 + k_1(x_1) + k_2(x_2) + \ldots + k_n(x_n) \tag{3}$$

where k_0 is the intercept, and n is the number of predictors, herein refers to precipitation and temperature, so $n = 2$ in this study. Preliminary analysis indicated 1-month lag between vegetation productivity and climatic variables, so we used

August sNDVI as the predictand, July precipitation and temperature as the predictors. The x_n and k_n are predictors and regression coefficients estimated using the simple least-squares technique (Gong and Shi 2003). x_1 and x_2 indicate precipitation and temperature, respectively.

ANN-GA model

Figure 2 shows the structure of the ANN-GA model for predicting the sNDVI. It is called ANN-GA because a GA is used to calibrate the parameters of an ANN (Kuo et al. 2010). ANN has a forward three-layer structure consisting of input, hidden, and output layer, with two nodes (precipitation and temperature) in the input layer, five neurons in the hidden layer, and one node (sNDVI) in the output layer. The number of input nodes is two for precipitation and temperature, and the output node is sNDVI. GA is used to optimize the model parameters for the different layers by minimizing an objective function and maximizing the correlation coefficients between observed and predicted sNDVI. The solution space is represented according to the finite lengths of strings called chromosomes, and the solution is improved iteratively using a combination of crossover and mutation (Kuo et al. 2010; Mwale and Gan 2005).

As a global optimization algorithm, the GA has a three-stage operation structure including selection, crossover, and mutation. At the selection stage, an initial set of weights (W) and biases (B) are randomly generated to produce an initial population with diverse information. The initial population size in this study is 200. All the neural networks considered are ranked in a descending order from the best to the worst performing neural networks according to their respective performances evaluated using the objective function values. Typically, only the top 85 % of the ranked neural networks are selected to generate offspring for the next generation. At the crossover stage, weights and biases of neural networks pairs selected from the population are exchanged using a one-point crossover method. This procedure is repeated between all pairs of neural networks in the selected population. At the mutation stage, mutation is implemented to restore good

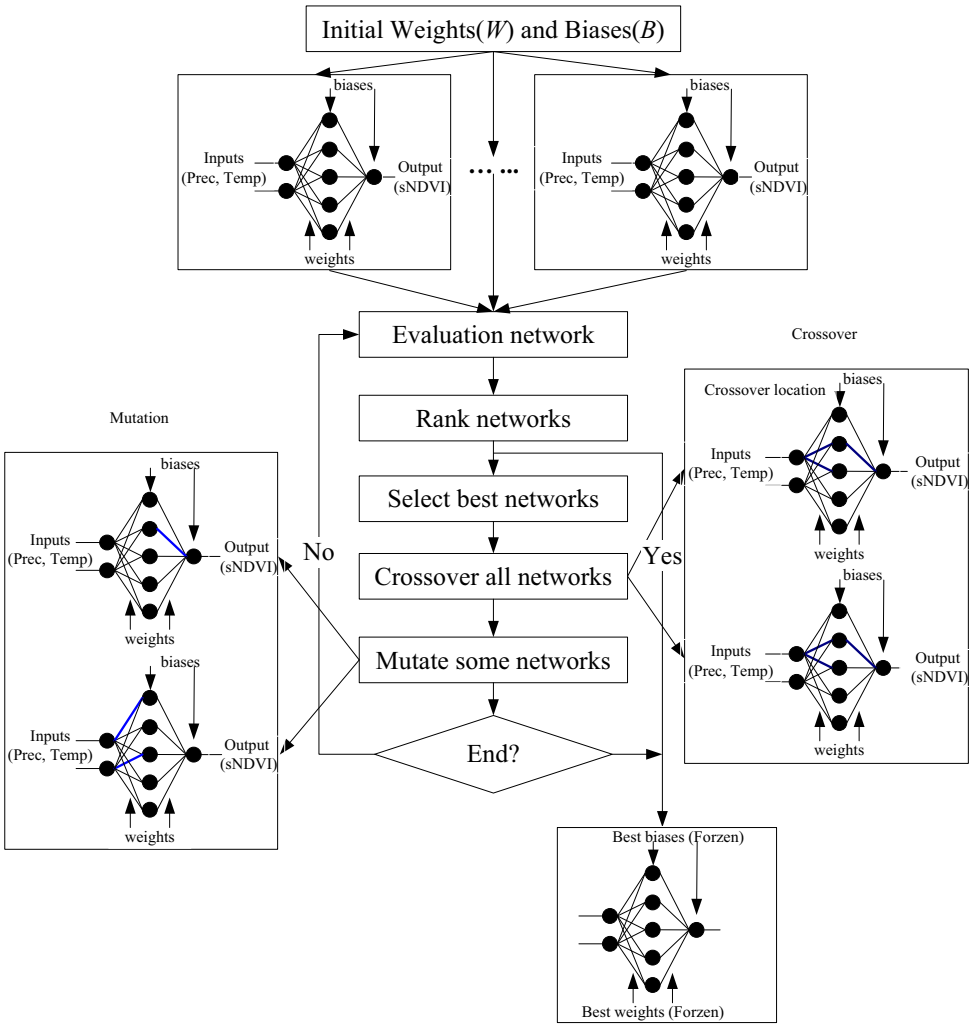

Fig. 2 Flowchart of the artificial neural network calibrated by the genetic algorithm (ANN-GA) model

weights and biases which are eliminated at the crossover stage. Only a small proportion (less than 1 %) of the total neural networks is retained for random mutation. The above three operations are repeated for many generations until more than 95 % of the converged neural networks have equal weights and biases. The weights and biases of the best remaining neural networks are used for predicting sNDVI (Mwale et al. 2004).

Pearson's correlation coefficient (ρ, Eq. 4) and root-mean-square error (RMSE, Eq. 5) are used to evaluate the performances of two predictive models. Bigger ρ and smaller RMSE indicate better predictive performances of predictive models.

$$\rho = \frac{\sum_{i=1}^{n}\left(P_i-\overline{P_i}\right)\left(O_i-\overline{O_i}\right)}{\sqrt{\sum_{i=1}^{n}\left(P_i-\overline{P_i}\right)^2}\times\sqrt{\sum_{i=1}^{n}\left(O_i-\overline{O_i}\right)^2}},\quad \rho\in[-1,1] \tag{4}$$

$$\mathrm{RMSE} = \sqrt{\sum_{i=1}^{n}\left(P_i-O_i\right)^2/n} \tag{5}$$

where P_i and O_i are the ith predicted and observed sNDVI, and $\overline{P_i}$ and $\overline{O_i}$ are their mean values, n is the sample size. More details of ρ and RMSE can be found in Albergel et al. (2013) and Kuo et al. (2010).

Results and discussion

Monthly variations of sNDVI and climatic variables

Figure 3 shows the 30-year (1982–2011) monthly mean values and trend magnitudes of sNDVI (Fig. 3a), precipitation (Fig. 3b), and temperature (Fig. 3c), and the correlation coefficients between sNDVI and precipitation (temperature) (Fig. 3d). Monthly sNDVI and its pattern were similar to those

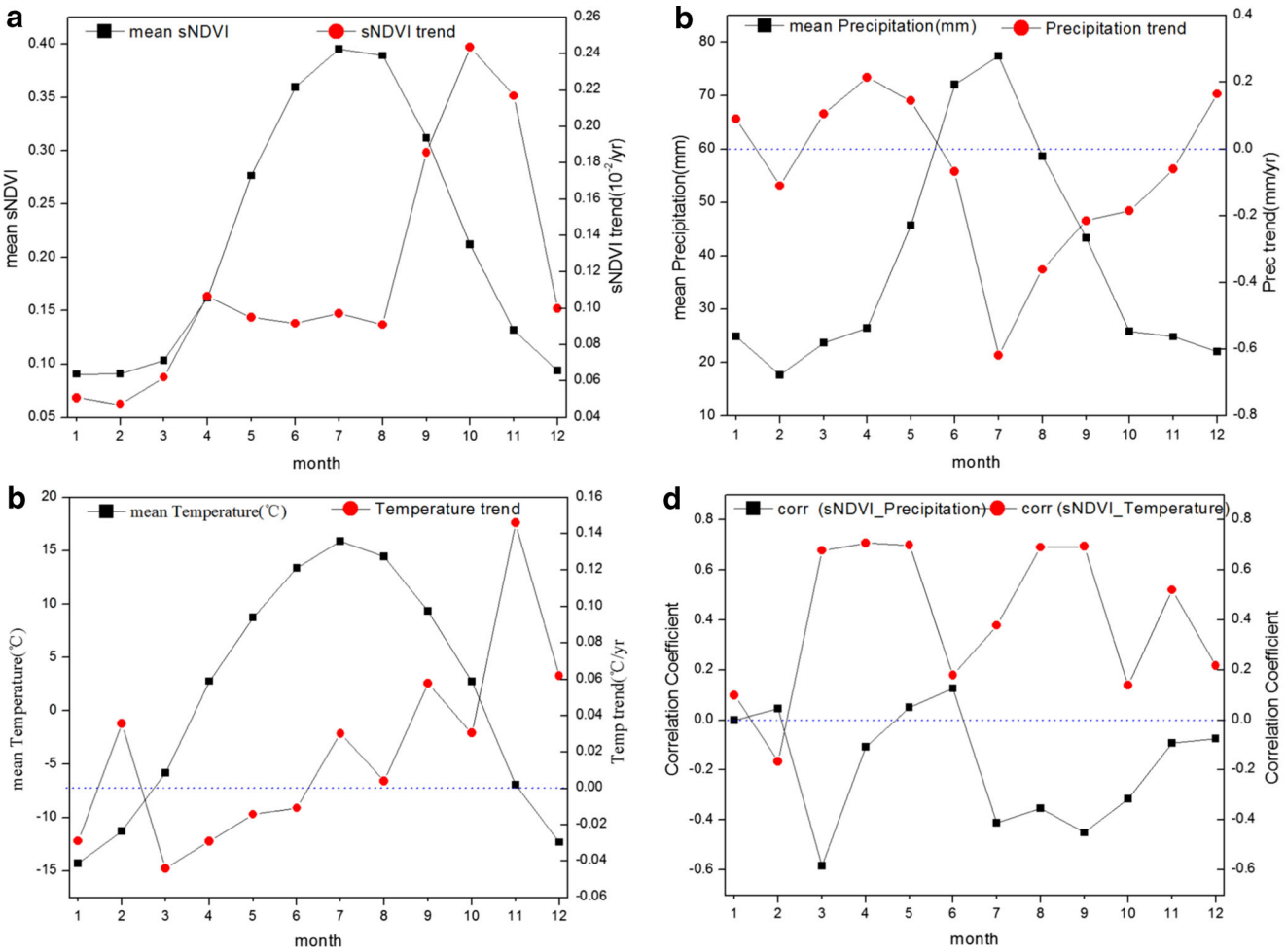

Fig. 3 Thirty-year mean values and trend magnitudes of monthly smoothed NDVI (sNDVI) and climatic variables from 1982 to 2011 in Alberta. **a** 30-year mean monthly sNDVI and trend magnitudes; **b** 30-year mean monthly precipitation and trend magnitudes; **c** 30-year mean monthly temperature and trend magnitudes; and **d** correlation coefficients ρ between monthly sNDVI and monthly precipitation (temperature)

of climatic variables. The largest value of mean sNDVI was detected in July (0.3954), and sNDVI of winter season (from December to February) were smaller (from 0.0905 to 0.0938) than other seasons for the period of 1982–2011. The slopes of monthly sNDVI trend were positive for all months, indicating that the sNDVI had increased over the 30-year period, and the largest slope was detected in October, which indicated a lengthened growing season or delayed winter. The results concurred with those of Ichii et al. (2002) which showed that NDVI had increased in the northern middle and high latitudes caused by the temperature rise. Piao et al. (2003) also showed that photosynthetic activity had increased and the growing season had extended over the past few decades in the northern middle and high latitudes by investigating the variations of terrestrial vegetation productivity. Monthly precipitation and temperature showed similar patterns compared with sNDVI, with the greatest value in July (77.43 mm for precipitation and 15.87 °C for temperature), greater values in summer, and relatively small values in winter. However, both summer and fall precipitation showed negative trend magnitudes. The largest negative slope occurred in July, with an annual rate of −0.62 mm, indicating that July precipitation had decreased by 15.58 mm over the period 1982 to 2011 (Fig. 3b), which echoed the inter- and intra-annual redistribution of precipitation as reported by IPCC (2013). The largest slope of monthly temperature was detected in November with an annual rate of 0.15 °C, which indicated that Alberta's mean temperature in November had increased up to 4.5 °C over the past 30 years. However, the slopes of temperature were negative from March to June (Fig. 3c), which indicated that the warming trends had slowed down, especially during spring. Previous study found that the annual mean temperature in Canada had increased by about 0.15 °C, and the greatest increasing trend of temperature had occurred during the winter for the period of 1950–2010 in Canada. However, a number of stations showed decreasing trends of summer temperature in the Canadian Prairies including Alberta, Manitoba, and Saskatchewan provinces (Vincent et al. 2012).

It is important for the satellite-based plant phenology analysis in view of the difference of NDVI values between the beginning and end of growing season. Assuming 5 °C as the threshold of growing season, the duration of growing season in Alberta starts at about April and ends at approximate September, lasting about 5 months. The corresponding sNDVI values were about 0.2 (at the beginning of growing season) and 0.25 (at the end of growing season), which are consistent with results of Piao et al. (2003) and Mao et al. (2012). From Fig. 3a, we detected that vegetation productivity peaked in the middle of the growing season (summer). The relatively large sNDVI increase occurred in the later growing season (fall). The largest slope of sNDVI occurred in October (+0.0024 per year), indicating that sNDVI in October had increased about 0.07 for the past 30 years in Alberta, followed by two adjacent months, November (+0.0022 per year) and September (+0.0019 per year), which indicated that the growing season had lengthened during the past 30 years. A trend of earlier vegetation greening in the spring had been detected in many regions from the satellite observations since early 1980s. Global warming might be one of the causes of the widespread lengthening of the growing season during recent decades. Vegetation productivity had improved because the photosynthetic activity had increased either by an earlier or by a lengthening of the growing season over the past few decades due to warming caused by climate change, especially at the northern middle and high latitudes (Barichivich et al. 2014; Neigh et al. 2007; Piao et al. 2003).

Figure 3d shows the correlation coefficients between monthly sNDVI and monthly precipitation (temperature), respectively. For temperature, all months except February exhibited positive correlation coefficients and strong positive correlation coefficients mainly occurred in spring (March, April, and May), August, and September. Both sNDVI and temperature showed large trend magnitudes in fall (Fig. 3a, c), indicating that increasing temperature could enhance vegetation productivity. A statistically meaningful relation between changes in NDVI and temperature increase for vegetated areas was detected by Zhou et al. (2001), which suggested that the relationship between vegetation productivity and temperature varied at different spatial and temporal scales. Kawabata et al. (2001) investigated the climate change impacts on the inter-annual variations of NDVI, and the results showed that vegetation activities had increased due to a gradual temperature rise in the northern middle and high latitudes. On the other hand, the correlation coefficients between sNDVI and precipitation fluctuated over the year for the period of 1982–2011. Generally, sNDVI in two third of the months had negatively correlated to precipitation. Correlation coefficients were relatively small in winter, during which time most of the vegetated areas were covered by the snow pack in Alberta and the impacts of precipitation on vegetation productivity were relatively weak. Figure 3d indicates that sNDVI-temperature correlations are stronger than those of sNDVI-precipitation, and temperature is considered to have the dominant influence on vegetation productivity in Alberta. A comparison of sNDVI trends (Fig. 3a) and sNDVI-climate correlations (Fig. 3d) indicated that sNDVI changes were mainly dominated by temperature rise and precipitation decrease in Alberta, especially during growing season. More details on the increasing trends of sNDVI will be provided by investigating trends of summer sNDVI for each individual grid points in Alberta in the following section. The strong correlations of sNDVI-climate relationships provided the

basic for sNDVI prediction using precipitation and temperature as predictors.

Spatiotemporal variability of summer sNDVI and correlation analysis

Figure 4 shows the spatial patterns of trend magnitudes of summer sNDVI for the period of 1982–2011 in Alberta. We especially focused on summer because it is in the middle of growing season, which had maximum sNDVI over the years investigated. As shown in Fig. 4, a high degree of spatial variability of summer sNDVI had been detected, and the spatial patterns of trend magnitudes were scattered. Most of the grid points (nearly 70 %) showed no significant trends at 5 % significant level, and the percentage of grid points with significantly increasing trend was about 20 %, while the rest of grid points (approximately 10 %) exhibited significantly decreasing trends. Significantly positive trends of summer sNDVI had mainly distributed in the south, parts of northeast and central Alberta, and areas along the Canadian Rocky Mountains. The largest slope was nearly 0.012 per year, which showed that sNDVI had increased about 0.36 over the past 30 years. Using AVHRR satellite data, Pouliot et al. (2009) evaluated the NDVI trends for the period of 1985–2006 in Canada, and the results showed that 22 % of the vegetated area of Canada had an increasing NDVI trend.

Figure 5 shows the temporal series of mean summer sNDVI, total summer precipitation, and mean summer temperature for the period of 1982–2011 in Alberta. The results indicated that summer sNDVI had been jointly influenced by both precipitation and temperature, e.g., summer sNDVI decreased when precipitation and temperature decreased from 1984 to 1988, and vice versa. Summer sNDVI was generally positively correlated to summer temperature, e.g., summer sNDVI increased from 1982 to 1984 and exhibited a modest decrease followed by a strong increasing trend until 1990, which might be due to the temperature rise for the periods of 1982–1984 and 1988–1989, and fluctuating anomalies between 1984 and 1988. The similar summer sNDVI anomalies had also occurred during 1991–1997 and 2000–2004. However, the relationships between summer sNDVI and precipitation were more complex than between summer sNDVI and temperature. Low negative correlations between summer sNDVI and precipitation had been detected. The complex relationships between summer sNDVI and

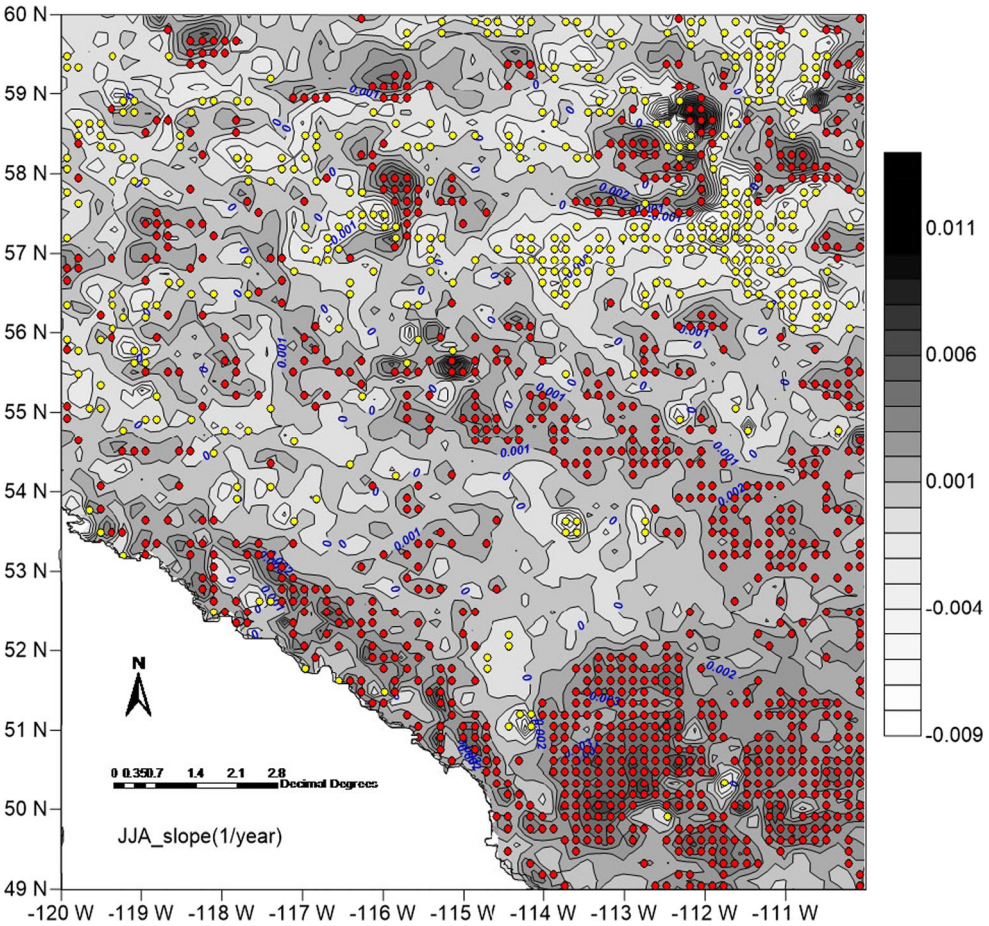

Fig. 4 Spatial patterns of trend magnitudes of summer sNDVI for the period of 1982–2011 in Alberta. The *grid points with red dot* have significantly increasing trends at 5 % significant level, and the *grid points with yellow dot* have significantly decreasing trends at 5 % significant level

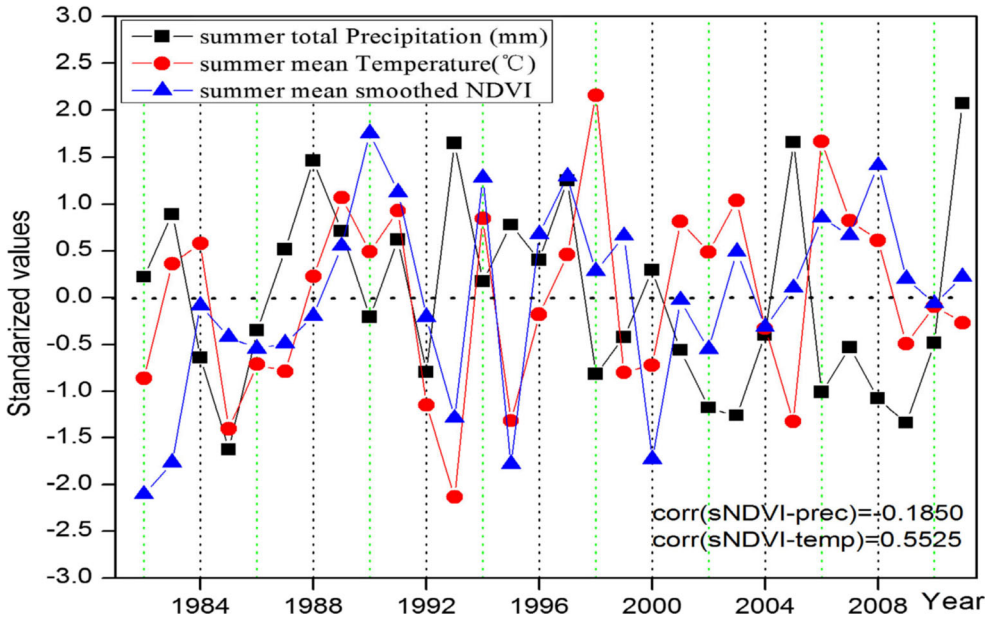

Fig. 5 Temporal series of mean summer sNDVI, total summer precipitation, and mean summer temperature for the period of 1982–2011 in Alberta

precipitation (temperature) might be caused by the complexity and variability of precipitation and temperature. Other climatic variables, such as soil moisture and solar radiation, and human activity also have influences on sNDVI.

Figure 6 shows the spatial patterns of correlation coefficients between summer sNDVI and climatic variables (Fig. 6a for precipitation and Fig. 6b for temperature) for regridded data series from 1982 to 2011. The percentage of grid points with positive correlations between summer sNDVI and precipitation was 47 %, and a majority of grid points (83 %) showed positive correlations between summer sNDVI and temperature. Positive correlations between summer sNDVI and precipitation mainly occurred in the southern Alberta, and most of the negative correlations occurred in the central Alberta and regions along with the Canadian Rocky Mountains (Fig. 6a). Positive correlations between summer sNDVI and

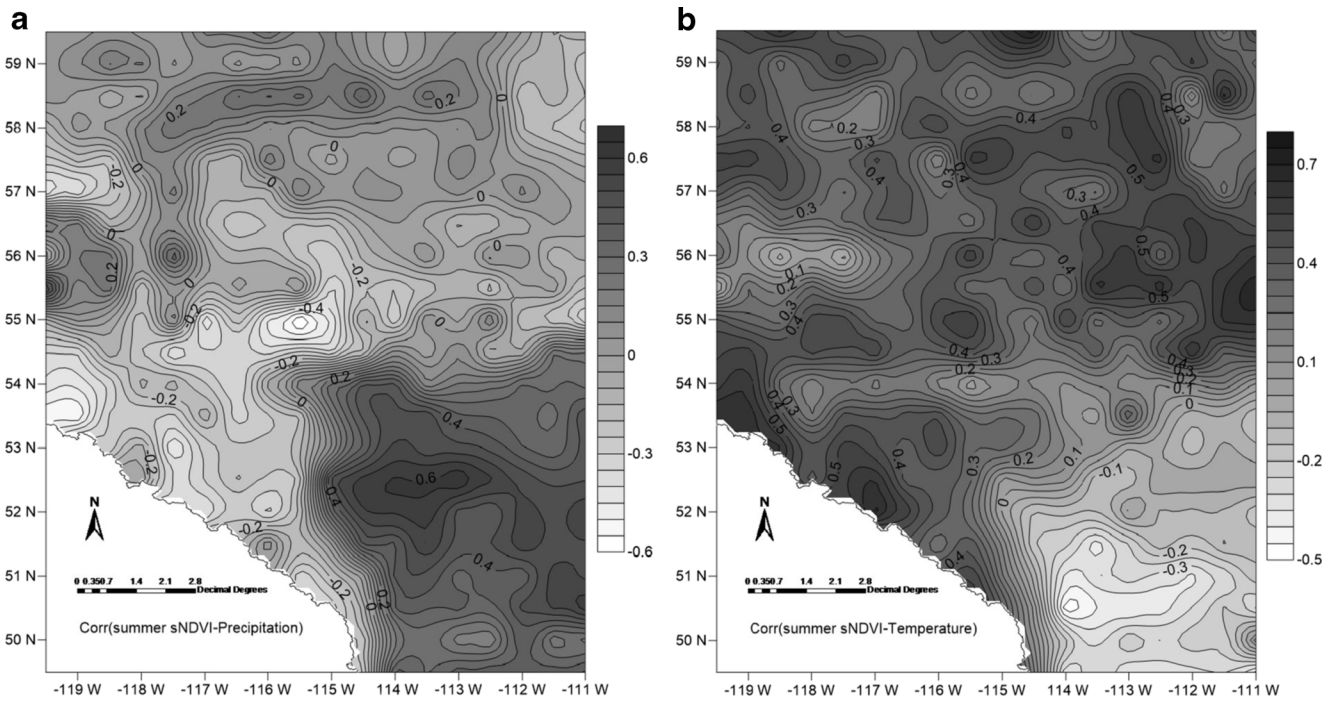

Fig. 6 Spatial patterns of correlation coefficients between summer sNDVI and climatic variables: **a** precipitation and **b** temperature for the period of 1982–2011 in Alberta

temperature had been detected in most areas of northern and central Alberta, whereas negative correlations had been mainly found in the southern Alberta (Fig. 6b). In the southern Alberta, precipitation increase and temperature decrease could raise the moisture availability for vegetation, leading to an increase of sNDVI. Ichii et al. (2002) concluded that the areas with negative correlations between NDVI and temperature coincided well with positive correlations between NDVI and precipitation, which mainly occurred in semiarid regions, where interannual NDVI variations had been determined by both precipitation and temperature.

Predictability of sNDVI

The multivariate linear regression and ANN-GA models have been used to predict August sNDVI for all grid points in Alberta, and the results showed that the grid points in the southeast of Alberta had better predictive performances than grid points in other regions of Alberta. The results were expected because stronger correlations between August sNDVI and July precipitation (temperature) were detected in the southeast of Alberta than other regions (Fig. 6). Given the predictive performances of grid points in the southeast of Alberta were

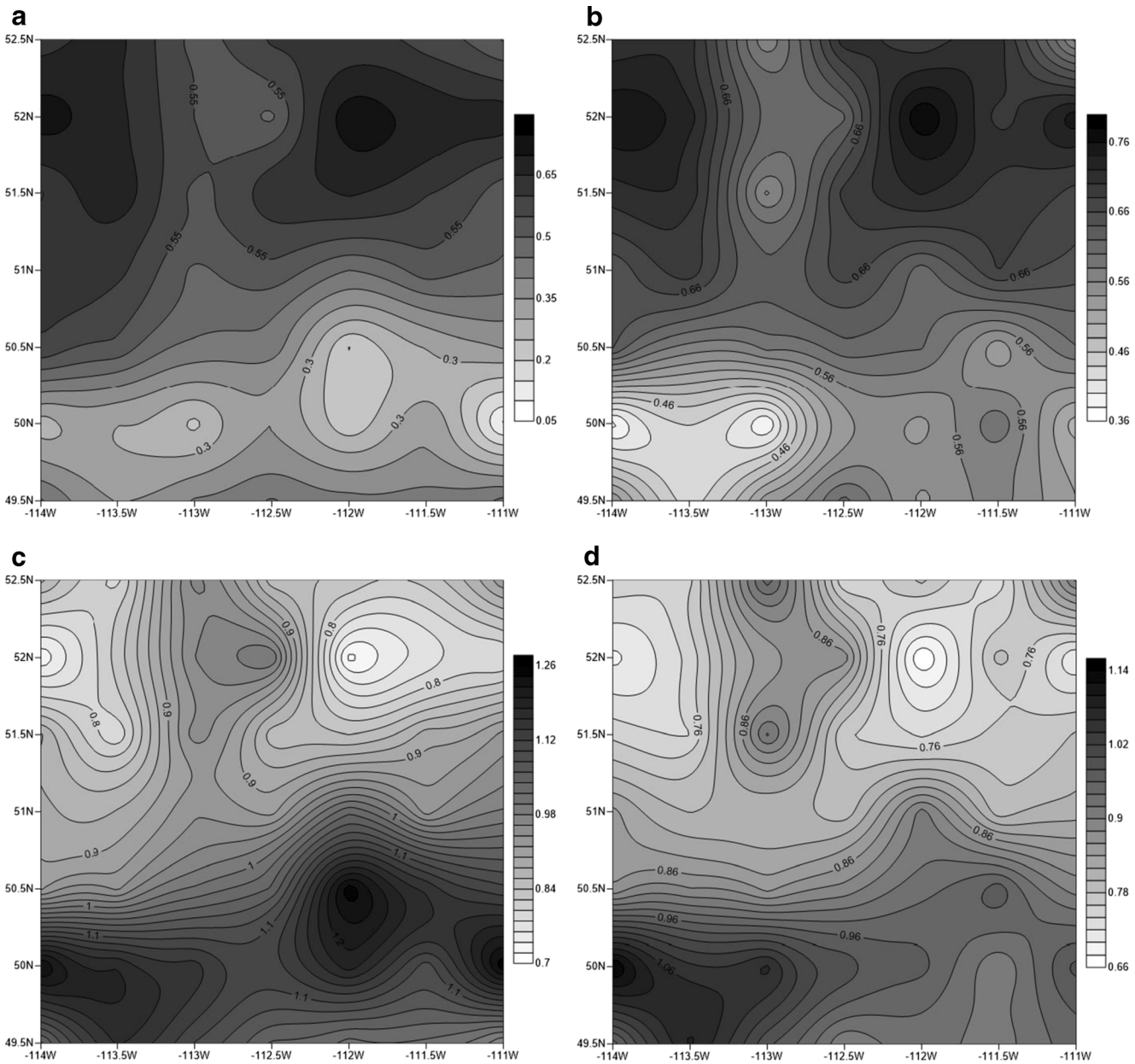

Fig. 7 Spatial patterns of predictive performances of two predictive models: **a** ρ for linear regression model; **b** ρ for ANN-GA model; **c** RMSE for linear regression model; and **d** RMSE for ANN-GA model to predict August sNDVI for the periods of 1982–2011 in the southeast of Alberta

better than other regions, we used grid points located in the southeast of Alberta to investigate which model and where the models should be more applicable. Figure 7 shows the spatial patterns of predictive performances including ρ and RMSE for both predictive models for grid points located in the southeast of Alberta (Fig. 7a ρ for linear regression model, Fig. 7b ρ for ANN-GA model, Fig. 7c RMSE for linear regression model, and Fig. 7d RMSE for ANN-GA model). Generally, the ANN-GA model exhibited better predictive performances (bigger ρ and smaller RMSE) between observed and predicted August sNDVI than using linear regression model (Fig. 7b). The ρ ranged from 0.372 to 0.781 for ANN-GA model and from 0.09 to 0.737 for linear regression model, while the RMSE ranged from 0.66 to 1.145 for ANN-GA model and from 0.713 to 1.256 for linear regression model. In

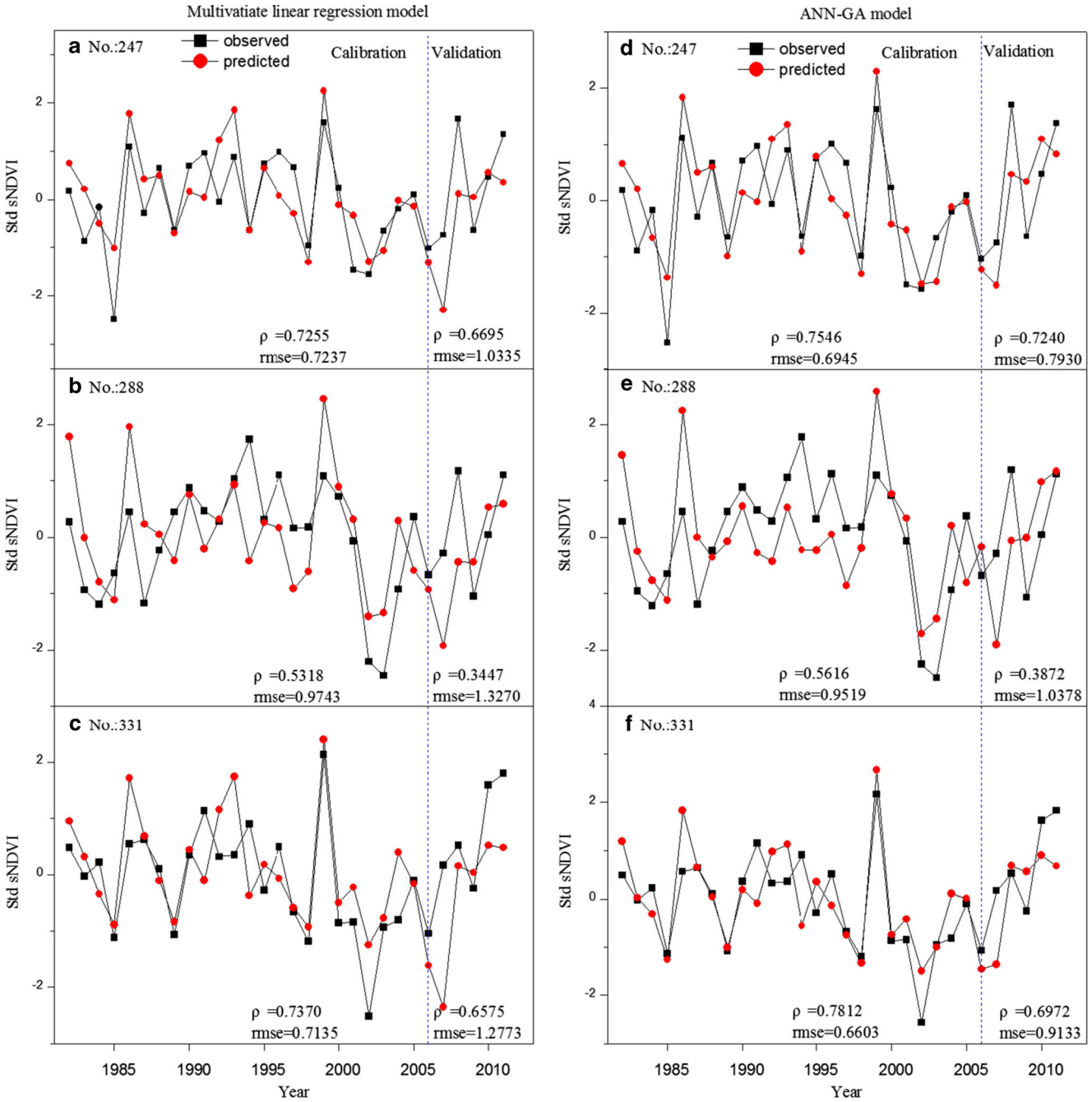

Fig. 8 The observed and predicted August sNDVI for three grid points (#247, #288, and #331) in the southeast of Alberta. The results of linear regression model are presented in **a**~**c** for grid points #247, #288, and #331, respectively, and the results of ANN-GA model are presented in **d**~**f** for grid points #247, #288, and #331, respectively. The predictive performances (ρ and RMSE) are given in each figure at both calibration stage (1982–2005) and validation stage (2006–2011)

the spatial scale, the results showed that the gird points located between 51°N-52.5°N latitude and 110°W-112.5°W, 113.5°W-114°W longitude had better predictive performances than grid points located in other areas, which was also expected because the correlation coefficients between August sNDVI and July precipitation (temperature) of those grid points were bigger than others.

Three typical grid points including #247 (−114°W, 52.5°N), #288 (−113°W, 52.5°N), and #331 (−112°W, 52°N) in the southeast of Alberta had selected to provide more details of the predictive performances of the linear regression model (Fig. 8a~c) and ANN-GA model (Fig. 8d–f). In general, better predictive performances had been detected for grid points #247 and #331 than grid point #288 because the correlation coefficients of grid points #247 and #331 between August sNDVI and July precipitation (temperature) were bigger than those of grid point #288. The ANN-GA model had better predictive performances (bigger ρ and smaller RMSE) than using linear regression model at both calibration and validation stages. At calibration stage, ρ between the observed and predicted August sNDVI ranged from 0.5318 to 0.7270 for linear regression model and from 0.5616 to 0.7812 for ANN-GA model. The RMSE between the observed and predicted August sNDVI ranged from 0.7135 to 0.9743 for linear regression model and from 0.6603 to 0.6945 for ANN-GA model. At validation stage, ρ between observed and predicted August sNDVI ranged from 0.3447 to 0.7240, and the RMSE ranged from 0.7930 to 1.3270 for both models. For grid point #247, correlation coefficients between the observed and predicted August sNDVI were 0.7546 and 0.7240 at calibration and validation stages using the ANN-GA model, respectively, but they dropped to 0.7255 and 0.6695 at both stages using linear regression model. The values of RMSE had increased to 0.7240 and 1.0335 using the linear regression model with respect to 0.6945 and 0.7930 of the ANN-GA model at both calibration and validation stages. For grid point #288, smaller ρ and bigger RMSE between the observed and predicted August sNDVI had been detected, with respect to the predictive performances of grid point #247 and #331, and the lowest ρ (0.3447) and the highest RMSE (1.3270) had been found. For grid point #331, correlation coefficients between observed and predicted August sNDVI using ANN-GA model were larger than using the linear regression model at both calibration and validation stages, and vice versa for RMSE.

From Figs. 7 and 8, we conclude that both ANN-GA and linear regression models can be used to predict sNDVI using precipitation and temperature as predictors based on the strong correlations of sNDVI-climate relationships. Considering some ecologists might focus on the vegetation productivity for different period, e.g., summer, we further investigated the possibility to predict summer sNDVI using precipitation and temperature as predictors. Again, we selected three typical grid points including #247, #288, and #331 based on the correlation coefficients between summer sNDVI and climatic variables. We did not test all the grid points in the southeast of Alberta because summer sNDVI weakly correlated to climatic variables for some grid points, which should not be suitable for summer sNDVI prediction, as shown in Fig. 6. Table 1 shows the predictive performances of three typical grid points (#247, #288, and #331) for both ANN-GA and linear regression models to predict summer sNDVI using precipitation and temperature as predictors over the period of 1982–2011 in the southeast of Alberta. The results were similar with those in Figs. 7 and 8. The ANN-GA model had better predictive performances (bigger ρ and smaller RMSE) than using linear regression model. Taking grid point #288 for an example, the ρ of ANN-GA model (0.675) is bigger than ρ of linear regression model (0.455), while the RMSE of ANN-GA model (0.799) is smaller than RMSE of linear regression model (1.019). The grid point #247 exhibited better predictive performances that grid points #288 and #331, which was also expected, because the correlation coefficients of grid point #247 between summer sNDVI and precipitation (temperature) were bigger that those of grid points #288 and #331.

To reveal the reason of ANN-GA model exhibited better predictive performances than linear regression model (as shown in Figs. 7 and 8), we investigated the scatter plots between July precipitation and temperature (predictors) and August sNDVI (predictands) for grid points #247, #288, and #331 in the southeast of Alberta. Figure 9 shows nonlinear relationships between August sNDVI and July precipitation (temperature), which

Table 1 Predictive performances of three typical grid points (#247, #288, and #331) for both ANN-GA and linear regression models to predict summer sNDVI over the period of 1982–2011 in the southeast of Alberta

Grid no.	Location		ANN-GA model		Linear regression model	
	Longitude	Latitude	ρ	RMSE	ρ	RMSE
#247	−114°W	52.5°N	0.694	0.784	0.674	0.870
#288	−113°W	52.5°N	0.675	0.799	0.455	1.019
#331	−112°W	52°N	0.549	0.977	0.463	1.071

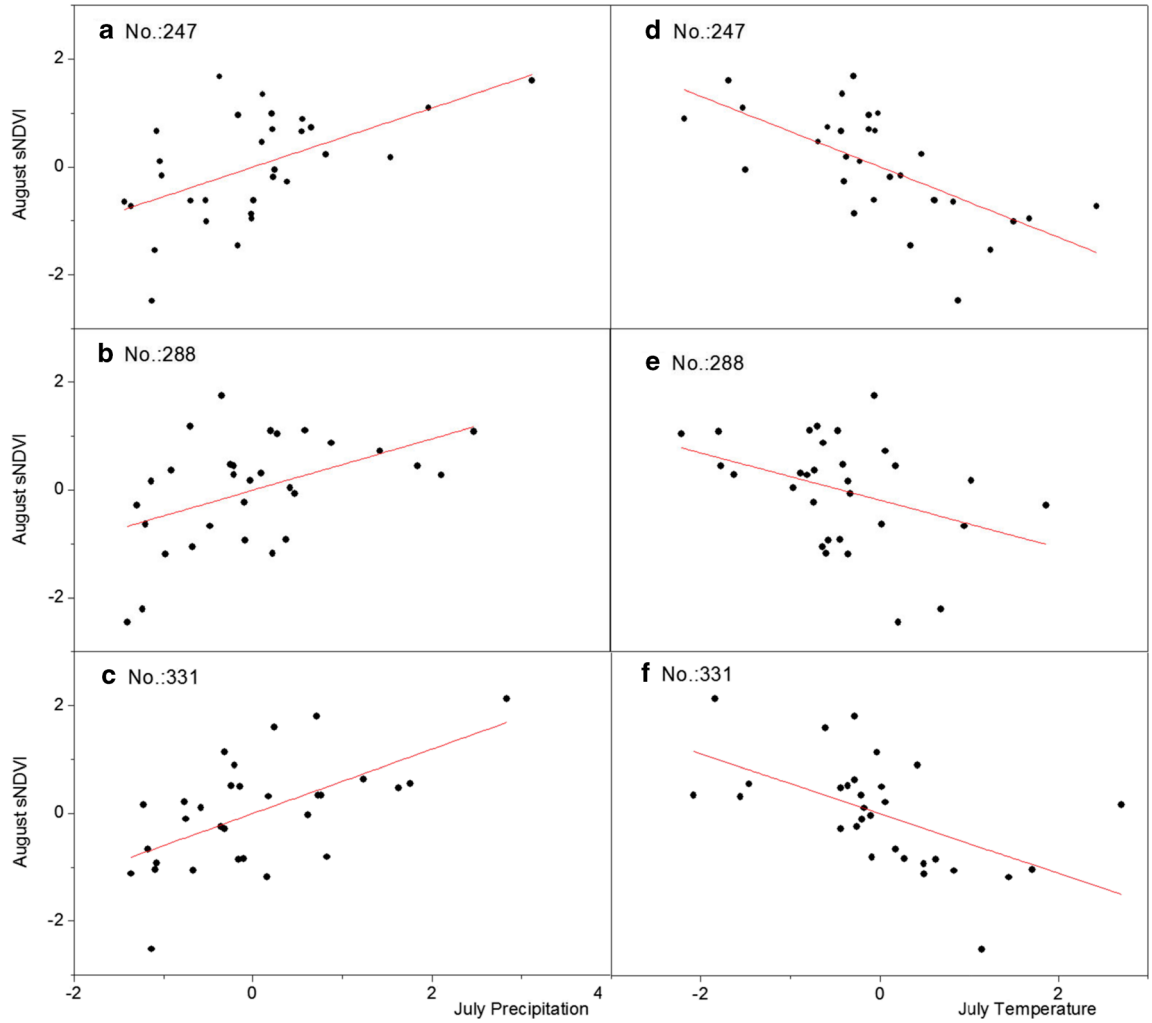

Fig. 9 Scatter plots of the August sNDVI and July climatic variables (precipitation and temperature) for three typical grid points. **a**~**c** August sNDVI and July precipitation for grid points #247, #288, and #331, respectively. **d**~**f** August sNDVI and July temperature for grid points #247, #288, and #331, respectively

implied that a nonlinear model (e.g., the ANN-GA model) should be more suitable than a linear model (e.g., linear regression model) for modeling the sNDVI-climatic relationships of Alberta. However, precipitation and temperature explained variances of between 30 and 43 % (i.e., ρ of 0.548 and −0.656) (Mwale et al. 2007), it is still a challenge calibrating the ANN-GA model even though it is a nonlinear model (Kuo et al. 2010). More climatic variables might improve the predictive performances, as found by Jahan and Gan (2011) which used two vegetation indices including NDVI and Enhanced Vegetation Index (EVI) from Moderate-resolution Imaging Spectroradiometer (MODIS) to monitor temporal responses of vegetation to climate over a boreal forest of western Canada. The results demonstrated a potential for monitoring the patterns of terrestrial vegetation productivity using climatic variables. They also found that the predictive performances were better using multiple climatic variables than using a single climatic variable as predictors to predict vegetation indices for a boreal mixed wood forest of western Canada.

Summary and conclusions

Using Mann-Kendall, Thiel-Sen slope, correlation analysis, linear regression, and ANN-GA, this study investigated the monthly variations of sNDVI and climatic variables (precipitation and temperature) and their relationships, based on which we studied the spatial patterns of trend magnitudes of summer sNDVI and correlations between summer sNDVI and climatic variables over the period of 1982–2011 in Alberta. Two models, linear regression and ANN-GA, were used to evaluate the potential predictability of August sNDVI using July precipitation and

temperature as predictors at 1-month lag time and summer sNDVI. Our findings are summarized as follows:

(1) In general, the sNDVI had increased over the past 30 years (Fig. 3a), especially from September to November, which indicated a lengthened growing season or delayed winter in Alberta. The pattern of monthly sNDVI was similar with monthly precipitation and temperature, with the biggest value in July, relatively bigger values in summer, and smaller values in winter. The correlations between monthly sNDVI and climatic variables (precipitation and temperature) varied from month to month, which suggested limited predictability of vegetation using precipitation and temperature as predictors (Fig. 3d).

(2) The spatial patterns of trend magnitudes for summer sNDVI were scattered. The percentages of grid points that showed significantly increasing trend, no significant trends, and significantly decreasing trend at 5 % significant level were approximately 20, 70, and 10 %, respectively. It seems that the trends of summer sNDVI are mainly associated with the trends of precipitation and temperature. Significant increasing trends mainly occurred in the southern Alberta, along Canadian Rockies, and parts of northeast Alberta (Fig. 4). The temporal series of mean summer sNDVI, total summer precipitation, and mean summer temperature indicated the complex relationships between sNDVI and climatic variables (Fig. 5). Summer sNDVI exhibited positive (negative) correlations with temperature (precipitation) in northern Alberta, and vice versa in southern Alberta (Fig. 6). Vegetation productivity in northern Alberta is mainly temperature driven and the vegetation in southern Alberta is predominantly precipitation driven. Temperature increase and precipitation decrease could promote the growth of vegetation. The precipitation decrease generally accompanied by an increasing incoming solar radiation.

(3) Two predictive models (linear regression and ANN-GA models) have been developed to predict August sNDVI using July precipitation (temperature) as predictors, to investigate the possible prediction of vegetation productivity using climatic variables. In general, the predictive performances differed for different areas and models. The ANN-GA model exhibited better predictive performances (bigger ρ and smaller RMSE) between observed and predicted August sNDVI than using linear regression model (Fig. 7), especially for gird points located between 51°N-52.5°N latitude and 110°W-112.5°W, 113.5°W-114°W longitude, where the sNDVI was stronger correlated to precipitation (temperature) than other areas. The results of August sNDVI for three grid points (#247, #288, and #331) provided more details of the predictive performances for both predictive models at both calibration and validation stages (Fig. 8). The scatter plots between August sNDVI and July precipitation (temperature) of grid points indicated that the nonlinear model was more suitable for modeling the NDVI and climatic variables relationships than linear model (Fig. 9). As demonstrated by Jahan and Gan (2011) and Zhang et al. (2007), human activity and other climatic variables (e.g., potential evapotranspiration, radiation, aridity index, and soil moisture) had important influences on vegetation growth. More climatic variables such as potential evapotranspiration, diurnal temperature range, and soil moisture may provide more insights, which will be explored in our future research. The similar results detected in the summer sNDVI prediction (Table 1) with those of August sNDVI prediction (Figs. 7 and 8) indicated that both ANN-GA model and linear regression models are applicative used to sNDVI for different period of year based on the strong correlations between sNDVI and climatic variables.

Acknowledgments The study was partly supported by the National Natural Science Foundation of China (Grant Nos. 51509201,41501231,51479160,41471451), Scientific Research Program Funded by Shaanxi Provincial Education Department (Grant No. 15JK1503), Research Foundation of State Key Laboratory Base of Eco-hydraulic Engineering in Arid Area (Grant No. 2013ZZKT-5), and Dr. Start-up Foundation of Xi'an University of Technology (Grant No. 118-211413). CANGRD data sets were provided by Ewa Milewska at the Climate Research Branch of the Meteorological Service of Canada. The weekly smoothed NDVI data is available at the NOAA's Satellite and Information Service (NRSDIS) (http://www.star.nesdis.noaa.gov/star/index.php). The authors thank Profs. Thian Yew Gan, Felix Kogan, and Dr. Xuezhi Tan for their assistance on this study. The valuable comments and suggestions of Prof. Scott C. Sheridan and two anonymous reviewers have greatly improved our manuscript.

References

Albergel C, Brocca L, Wagner W, De Rosnay P, et al. (2013) Chapter 18: selection of performance metrics for global soil moisture products: the case of ASCAT product. In: GP Petropoulos (Ed.), Remote sensing of land surface turbulent fluxes and soil surface moisture content: state of the art. Taylor & Francis (p. 562)

Barichivich J, Briffa KR, Myneni R et al (2014) Temperature and snow-mediated moisture controls of summer photosynthetic activity in northern terrestrial ecosystems between 1982 and 2011. Remote Sens 6:1390–1431

Bayazit M, Önöz B (2007) To prewhiten or not to prewhiten in trend analysis? Hydrol Sci J 52:611–624

Canon J, Dominguez F, Valdes JB (2011) Vegetation responses to precipitation and temperature: a spatiotemporal analysis of ecoregions in the Colorado River Basin. Int J Remote Sens 32:5665–5687

Chuai XW, Huang XJ, Wang WJ, Bao G (2012) NDVI, temperature and precipitation changes and their relationships with different

vegetation types during 1998–2007 in Inner Mongolia, China. Int J Climatol 33:1696–1706

de Jong R, de Bruin S, de Wit A, Schaepman ME, Dent DL (2011) Analysis of monotonic greening and browning trends from global NDVI time-series. Remote Sens Environ 115:692–702

Dorigo WA, Zurita-Milla R, de Wit AJW et al (2007) A review on reflective remote sensing and data assimilation techniques for enhanced agroecosystem modeling. Int J Appl Earth Obs Geoinf 9:165–193

Dorigo W, De Jeu R, Chung D et al (2012) Evaluating global trends (1988–2010) in homogenized remotely sensed surface soil moisture. Geophys Res Lett 39:L18405

Gan TY (1998) Hydroclimatic trends and possible climatic warming in the Canadian Prairies. Water Resour Res 34:3009–3015

Gómez-Mendoza L, Galicia L, Cuevas-Fernández ML et al (2008) Assessing onset and length of greening period in six vegetation types in Oaxaca, Mexico, using NDVI-precipitation relationships. Int J Biometeorol 52:511–520

Gong DY, Shi PJ (2003) Northern hemispheric NDVI variations associated with large-scale climate indices in spring. Int J Remote Sens 24: 2559–2566

Gordon S, Wiebe H, Jacksteit R, Bennett S (2005) Water resources management and the energy industry in Alberta, Canada. J Can Pet Technol 44:22–27

Hopkinson RF, Hutchinson MF, McKenney DW, Milewska EJ, Papadopol P (2012) Optimizing input data for gridding climate normals for Canada. J Appl Meteorol Climatol 51:1508–1518

Ichii K, Kawabata A, Yamaguchi Y (2002) Global correlation analysis for NDVI and climatic variables and NDVI trends: 1982–1990. Int J Remote Sens 23:3873–3878

IPCC (2013) Climate change 2013: the physical science basis. Contribution of working group I to the fifth assessment report of the intergovernmental panel on climate change, 2013

Jahan N, Gan TY (2011) Modelling the vegetation-climate relationship in a boreal mixedwood forest of Alberta using normalized difference and enhanced vegetation indices. Int J Remote Sens 32:313–335

Jiang R, Gan TY, Xie J, Wang N (2014) Spatiotemporal variability of Alberta's seasonal precipitation, their teleconnection with large-scale climate anomalies and sea surface temperature. Int J Climatol 34:2899–2917

Jiang R, Gan TY, Xie J, Wang N, Kuo CC (2015) Historical and potential changes of precipitation and temperature of Alberta subjected to climate change impact: 1900–2100. Theor Appl Climatol, 1-15, doi: 10.1007/s00704-015-1664-y

Kawabata A, Ichii K, Yamaguchi Y (2001) Global monitoring of interannual changes in vegetation activities using NDVI and its relationships to temperature and precipitation. Int J Remote Sens 22:1377–1382

Kogan F, Guo W, Jelenak A (2011) Global vegetation health: long-term data records. Use of satellite and in-situ data to improve sustainability. Springer, pp. 247–255

Kogan F, Adamenko T, Guo W (2013) Global and regional drought dynamics in the climate warming era. Remote Sens Lett 4:364–372

Kuo CC, Gan TY, Yu PS (2010) Wavelet analysis on the variability, teleconnectivity, and predictability of the seasonal rainfall of Taiwan. Mon Weather Rev 138:162–175

Latifovic R, Trishchenko AP, Chen J, Park WB, Khlopenkov KV, Fernandes R, Pouliot D, Ungureanu C, Luo Y, Wang S, Davidson A, Cihlar J (2005) Generating historical AVHRR 1 km baseline satellite data records over Canada suitable for climate change studies. Can J Remote Sens 31:324–346

Mao D, Wang Z, Luo L, Ren C (2012) Integrating AVHRR and MODIS data to monitor NDVI changes and their relationships with climatic parameters in Northeast China. Int J Appl Earth Obs 18:528–536

Mekis E, Vincent LA (2011) An overview of the second generation adjusted daily precipitation dataset for trend analysis in Canada. Atmosphere-Ocean 49:163–177

Mwale D, Gan TY (2005) Wavelet analysis of variability, teleconnectivity, and predictability of the September-November East African rainfall. J Appl Meteorol 44:256–269

Mwale D, Gan TY, Shen SSP (2004) A new analysis of variability and predictability of seasonal rainfall of central southern Africa for 1950–94. Int J Climatol 24:1509–1530

Mwale D, Gan TY, Shen SSP, Shu TT, Kim KM (2007) Wavelet empirical orthogonal functions of space-time-frequency regimes and predictability of southern Africa summer rainfall. J Hydrol Eng 12: 513–523

Mwale D, Gan TY, Devito K, Mendoza C, Silins U, Petrone R (2009) Precipitation variability and its relationship to hydrologic variability in Alberta. Hydrol Process 23:3040–3056

Neigh CSR, Tucker CJ, Townshend JRG (2007) Synchronous NDVI and surface air temperature trends in Newfoundland: 1982 to 2003. Int J Remote Sens 28:2581–2598

Nemani RR, Keeling CD, Hashimoto H et al (2003) Climate-driven increases in global terrestrial net primary production from 1982 to 1999. Science 300:1560–1563

Piao S, Fang J, Zhou L, Guo Q, Henderson M, Ji W, Li Y, Tao S (2003) Interannual variations of monthly and seasonal normalized difference vegetation index (NDVI) in China from 1982 to 1999. J Geophys Res 108:4401

Piao SL, Ciais P, Huang Y, Shen ZH, Peng SS, Li JS, Zhou LP, Liu HY, Ma YC, Ding YH, Friedlingstein P, Liu CZ, Tan K, Yu YQ, Zhang TY, Fang JY (2010) The impacts of climate change on water resources and agriculture in China. Nature 467:43–51

Pouliot D, Latifovic R, Olthof I (2009) Trends in vegetation NDVI from 1 km AVHRR data over Canada for the period 1985–2006. Int J Remote Sens 30:149–168

Prasad VK, Anuradha E, Badarinath KVS (2005) Climatic controls of vegetation vigor in four contrasting forest types of India—evaluation from National Oceanic and Atmospheric Administration's Advanced Very High Resolution Radiometer datasets (1990–2000). Int J Biometeorol 50:6–16

Tanzeeba S, Gan TY (2012) Potential impact of climate change on the water availability of South Saskatchewan River Basin. Clim Chang 112:355–386

Vincent LA, Gullett DW (1999) Canadian historical and homogeneous temperature datasets for climate change analyses. Int J Climatol 19: 1375–1388

Vincent LA, Wang XLL, Milewska EJ, Wan H, Yang F, Swail V (2012) A second generation of homogenized Canadian monthly surface air temperature for climate trend analysis. J Geophys Res-Atmos 117

Wang J, Rich PM, Price KP (2003) Temporal responses of NDVI to precipitation and temperature in the central Great Plains, USA. Int J Remote Sens 24:2345–2364

Yue S, Pilon P, Phinney B, Cavadias G (2002) The influence of autocorrelation on the ability to detect trend in hydrological series. Hydrol Process 16:1807–1829

Zhang XB, Vincent LA, Hogg WD, Niitsoo A (2000) Temperature and precipitation trends in Canada during the 20th century. Atmosphere-Ocean 38:395–429

Zhang XB, Zwiers FW, Hegerl GC, Lambert FH, Gillett NP, Solomon S, Stott PA, Nozawa T (2007) Detection of human influence on twentieth-century precipitation trends. Nature 448:461–U464

Zhou LM, Tucker CJ, Kaufmann RK, Slayback D, Shabanov NV, Myneni RB (2001) Variations in northern vegetation activity inferred from satellite data of vegetation index during 1981 to 1999. J Geophys Res-Atmos 106:20069–20083